

Exploiting the Short-Term and Long-Term Channel Properties in Space and Time: Eigenbeamforming Concepts for the BS in WCDMA

CHRISTOPHER BRUNNER¹, WOLFGANG UTSCHICK, AND JOSEF A. NOSSEK
Institute for Circuit Theory and Signal Processing - Munich University of Technology, Germany
{brunner,utschick,nossek}@nws.ei.tum.de

Abstract. The deployment of adaptive antennas at base stations considerably increases the spectral efficiency of wireless communication systems. To reduce the computational complexity and increase performance of space-time (ST) processing, processing may take place in reduced dimension, i.e., pre-filtering takes place which is related to linear estimation theory based on second order statistics. To this end, long-term and short-term channel estimates are integrated into specific Tx/Rx systems. In this article, we present a new ST rake structure for uplink reception in WCDMA which operates in reduced dimension. Accordingly, our approach combines short-term and long-term spatial and temporal channel properties using an eigenanalysis. By choosing dominant eigenbeams in time and space, the algorithm enhances interference suppression as well as spatial and temporal receive diversity. In contrast to previously introduced well-known receiver structures, the ST eigenrake inherently adapts to different propagation environments and achieves higher spectral efficiency than other receivers. This is illustrated by Monte-Carlo simulations.

Then we extend the proposed concept to the downlink. The downlink eigenbeamformer improves closed-loop downlink diversity compared to other proposals in standardization (3GPP) which only exploit short-term channel properties. Even though the short-term feedback rate remains unchanged, additional antenna elements can be included to increase antenna and diversity gain. We also present a tracking solution to the downlink eigenbeamforming in WCDMA. To this end, we propose a distributed implementation of the eigenspace/-beam tracking at the mobile terminal and base station (BS), respectively. Moreover, the specific nature of the deployed tracking scheme offers an advantageous feedback signalling.

1 INTRODUCTION

The performance of digital mobile radio communication systems is limited by fast fading and interference from co-channel users. Let us recall that fading in the mobile radio channel occurs in two different time scales and, accordingly, can be classified into two different categories, namely short-term (small-scale, fast) fading and long-term (large-scale, slow) fading [1]:

- Short-term fading is due to scattering and/or reflections of the transmitted signals by surrounding objects. Short-term fading may cause rapid and large variations and is superimposed on top of long-term fading. Accordingly, the channel stays constant only during its coherence time.
- Long-term fading includes distance-related attenuation and slow shadow fading which is due to the ter-

rain, buildings, or other obstacles between transmitter and receiver. Long-term effects cause relatively slow variations of the (mean) signal as the mobile moves in space.

Long-term fading is easily compensated by power control [2], whereas both short-term fading and interference can be reduced by the use of antenna arrays at the base station with the appropriate signal processing, i.e., by combining and interference suppression. Therefore, adaptive antennas are an important technology to meet the high spectral efficiency and quality requirements of third generation (3G) mobile radio systems. W-CDMA [3] which is based on DS-SS-CDMA offers many degrees of freedom and, therefore, an easy and flexible implementation of new and more sophisticated services. Since this air interface also seems to become the most important of all 3G interfaces, we focus on W-CDMA. Of course, eigenbeamforming concepts also apply to TDMA or OFDM systems.

¹Now with ARRAYCOM, San Jose, USA.

In DS-CDMA systems using adaptive antennas, we have separation mechanisms in code and space. Our goal, therefore, is to support separation by code with separation in space when necessary, i.e., to use the degrees of freedom for beamforming efficiently. To this end, we can use optimum combining [4] in space and time which is equivalent with a ST Wiener filter or the ST MMSE approach, cf. also [5, 6, 7]. If the channel estimate is accurate, this approach is the best single-user linear detector² in terms of bit-error-ratio (BER). However, in DS-CDMA systems, the channel estimate of the weak taps typically is not accurate and, if the channel consists of many taps and several antennas, the measurement covariance matrices and the Wiener Hopf equations become rather large leading to a large computational complexity.

Two other well-known ST receiver structures for DS-CDMA systems are less computationally complex: the beamformer rake [9, 10, 6] and the maximum-ratio-combining (MRC) ST rake [5, 6]. Both receiver structures use the long-term temporal channel properties to select the dominant temporal taps or rake fingers with a conventional rake searcher. Based on these rake fingers, the MRC ST rake performs MRC in space whereas the beamformer rake determines the long-term spatial covariance matrices corresponding to the rake fingers and applies a spatial eigenfilter [11, 12, 10] to each of these taps, i.e. the dominant eigenvector is used for beamforming. In spatially coherent scenarios the beamformer rake shows a good performance. Since the long-term spatial covariance matrices can be estimated over many taps, the spatial filters are accurately estimated and, accordingly, full antenna gain is available for short-term channel estimation and symbol detection. However, if the scenario is spatially selective, performance degrades because spatial diversity is not available since only the strongest eigenvector is considered and, moreover, the strongest eigenvector will represent only a small part of the power of the corresponding channel tap. The performance of the MRC ST rake is opposite. Performance is bad for spatially coherent scenarios due to a degraded channel estimation. On the other hand, performance is good in spatially selective scenarios compared to the beamformer rake, since spatial diversity is exploited. Note, moreover, that the MRC ST rake does not consider colored interference. In this work, we discuss a space-time rake receiver structure, namely the space-time eigenrake, which avoids these disadvantages and outperforms previously discussed rake receivers at modest computational complexity by effectively exploiting the short-term and long-term channel properties in space and time. Moreover it has been shown that the space-time eigenrake matches the performance of the maximum-likelihood detector in reduced dimension,

²Multi-user detection (MUD) schemes [8] are not considered in the sequel. MUD schemes have limited influence on the spectral efficiency of the system considering uplink and downlink jointly since the downlink is the bottleneck in W-CDMA and MUD applies only in the uplink. Moreover, intercell interference is not suppressed and the computational complexity is very large especially if many users share the same channel.

if the low-rank radio channel is characterized by spatio-temporal taps which are disjoint both in space and time [13], cf. [14].

In the next step, we extend the concept of the space-time eigenrake to the downlink. On the downlink, the spatial processing³ is carried out prior to transmission and, therefore, *before* the signal encounters the channel. This considerably differs from uplink processing with adaptive antennas, where the spatial processing is performed *after* the channel has affected the signal. Clearly, the objective is to obtain an accurate short-term downlink channel estimate at the base station to be able to do downlink processing. In this work, we focus on feedback from the mobile terminal. However, the limited reciprocity between uplink and downlink in FDD systems [7, 15] which is restricted to long-term channel properties can be exploited as well. Consequently, various closed-loop Tx diversity concepts have been suggested in standardization (3GPP) for 2, 4, and > 4 antenna elements, respectively, which solely exploit short-term channel fluctuations [16, 17] or both consider short-term and long-term (spatial) channel properties [18, 19, 7]. The latter has become known as the *downlink eigenbeamforming* concept, which is based on a principal component analysis of the long-term spatial covariance matrices of the radio channel [18, 19, 20, 21].

This paper is organized as follows. After briefly reviewing several processing schemes in Section 2 in reduced dimension, we motivate the eigenbeamforming concept. Then eigenbeamforming is applied to the space-time receiver structure for the uplink in Section 3 and the performance is validated by Monte-Carlo simulations. In Section 4, we apply the eigenbeamforming concept to the downlink and show simulation results. Finally, Section 4.3 presents the tracking solution to the downlink eigenbeamforming and explains the specific nature of the deployed tracking scheme which offers an advantageous feedback signalling.

2 REDUCED DIMENSION PROCESSING

The main difference between previous proposals for reduced dimension processing and eigenbeamforming is that previous proposals do not exploit the long-term channel information and, therefore, are not using all available information. We will briefly review existing proposals before motivating eigenbeamforming.

Typically, reduced dimension processing helps solve linear equations more efficiently. In general, the short-term weight vector for data detection is obtained with a MMSE approach (Wiener filter, optimum combining) in CDMA

³In the sequel, downlink ST processing is separated between base station (BS) and mobile terminal, resp. mobile terminal, i.e., spatial processing takes place at the BS and a conventional rake receiver performs temporal processing at the mobile terminal.

systems. The Wiener-Hopf equation in the space-time domain yields

$$\mathbf{h}^{(ST)} = \mathbf{K}_X^{(ST)} \mathbf{w}^{(ST)} \in \mathbb{C}^{M \cdot N_w}, \quad (1)$$

where $\mathbf{h}^{(ST)}$, $\mathbf{K}_X^{(ST)}$, and $\mathbf{w}^{(ST)}$ denote the channel estimate, the short-term measurement covariance matrix, and the weight vector, all in space and time. Moreover, M is the number of antenna elements and N_w denotes the number of temporal taps. Due to the high chiprate in DS-CDMA systems compared with the symbol rate in GSM, the channel length in samples can be large. If, for instance, $M = 8$ antennas and $N_w = 20$ samples hold, we have 160 equations which have to be solved slotwise. In addition, the short-term measurement covariance matrix of dimension 160×160 has to be estimated correctly, for instance, by using a sliding window.

There are several methods to solve (1) in reduced dimension. In [22], we have introduced the space-frequency rake and applied it in the W-CDMA context. To this end, (1) is transformed into the space-frequency domain and weak frequency taps are dropped. Compared to the joint space-time rake⁴ performance gains are obtained only if oversampling takes place in time. Dimension reduction can be achieved in the spatial domain by performing a transformation into beamspace and dropping weak beams. Alternatively, (1) can be solved by using the auxiliary vector method [23] or the multistage Wiener filter approach [24] or iteratively by performing Gauss-Seidel iterations [25]. Several dimension reduction techniques are also discussed in [26] with a focus on reducing computational complexity for parameter estimation.

To motivate the eigenbeamforming concept, characteristics of the conventional time-only rake [27] are briefly discussed. The complete short-term channel estimate in time $\mathbf{h}^{(T)}(i) \in \mathbb{C}^{N_d}$ (of one antenna) can be obtained by correlation with the pilot sequence which is part of the control channel. Here, i and N_d denote the slot number and the maximum delay spread in samples, respectively. If $\mathbf{h}^{(T)}(i)$ is wide-sense-stationary (WSS) [28], the long-term temporal signal covariance matrix equals

$$\mathbf{R}_S^{(T)} = \mathbb{E}\{\mathbf{h}^{(T)}(i)(\mathbf{h}^{(T)}(i))^H\}. \quad (2)$$

Since uncorrelated scattering (US) [28] is assumed, $\mathbf{R}_S^{(T)}$ is diagonal and the contributions of temporal taps (rake fingers) selected for further processing steps are uncorrelated. More precisely, correlation between adjacent samples also depends on oversampling and on the chosen chip waveform. Therefore, adjacent taps are not selected by the rake searcher in case of an oversampling factor of $M_c = 2$. An example of a temporal covariance matrix is given in Figure 1. The correlations and, therefore, the computational complexity for short-term processing, which comprises short-term channel estimation and data detection, are

⁴Note, that in the sequel the notation *joint space-time rake* or *joint ST rake* is a synonym for the ST MMSE, ST Wiener filter, etc.

reduced considerably by taking into account only the dominant temporal taps. The selection of the dominant taps can occur in the long-term which means that operations may be spread over several slots and computational effort is very low. Moreover, data detection is improved since channel estimation of weak temporal taps is unreliable.

We would like to do something similar in space. Recall that the beamformer rake uses an eigenfilter for each dominant temporal tap which selects only the dominant eigenvector. Therefore, the diversity order obtained in space cannot exceed one and performance degrades in spatially selective scenarios. On the other hand, the maximum ratio combiner in space exploits spatial diversity but channel estimation deteriorates in spatially highly correlated scenarios in comparison to the eigenfilter approach. An example of a spatial covariance matrix is plotted in Figure 1 illustrating that we cannot simply drop the outputs of antenna elements. The spatial channel estimates $\mathbf{h}^{(S)}(i)$ (for one temporal tap) are correlated for most scenarios. The entries of the long-term spatial correlation matrix,

$$\mathbf{R}_S^{(S)} = \mathbb{E}\{\mathbf{h}^{(S)}(i)(\mathbf{h}^{(S)}(i))^H\} \quad (3)$$

depend on the spatial distribution of wave incidence power for the given temporal tap. Clearly, in contrast to dropping temporal taps, it is not recommendable to drop the output of some of the antenna elements to increase performance and reduce complexity. However, a similar approach can be applied after performing a transformation of spatial measurements. In order to find a suitable transformation, let us state two major goals:

- The transformed outputs should be as uncorrelated as possible in terms of the desired signal in order to maximize the diversity gain using a small number of spatial filters.
- The spread of the mean (long-term) signal to interference and noise ratio (SINR) of the transformed outputs should be maximized to maximize the interference suppression for a small number of spatial filters.

These goals are jointly optimized by carrying out a generalized eigenvalue decomposition of the long-term spatial correlation matrices⁵,

$$\mathbf{\Lambda} = \mathbf{W}^{(S),-1} \mathbf{R}_{IN}^{(S),-1} \mathbf{R}_S^{(S)} \mathbf{W}^{(S)}, \quad (4)$$

where

$$\mathbf{W}^{(S)} = \begin{bmatrix} \mathbf{w}_1^{(S)} & \mathbf{w}_2^{(S)} & \dots & \mathbf{w}_M^{(S)} \end{bmatrix}$$

denotes the eigenvectors and the diagonal matrix $\mathbf{\Lambda}$ contains the corresponding eigenvalues. The *spatial rake*

⁵Note that $\mathbf{R}_{IN}^{(S)}$ is estimated by averaging over the outer product of the spatial snapshots given by $\mathbf{x}(t)$, cf. (5). Since the signal of interest is significantly weaker than the sum of interfering signals in W-CDMA, it is not necessary to extract the signal part.

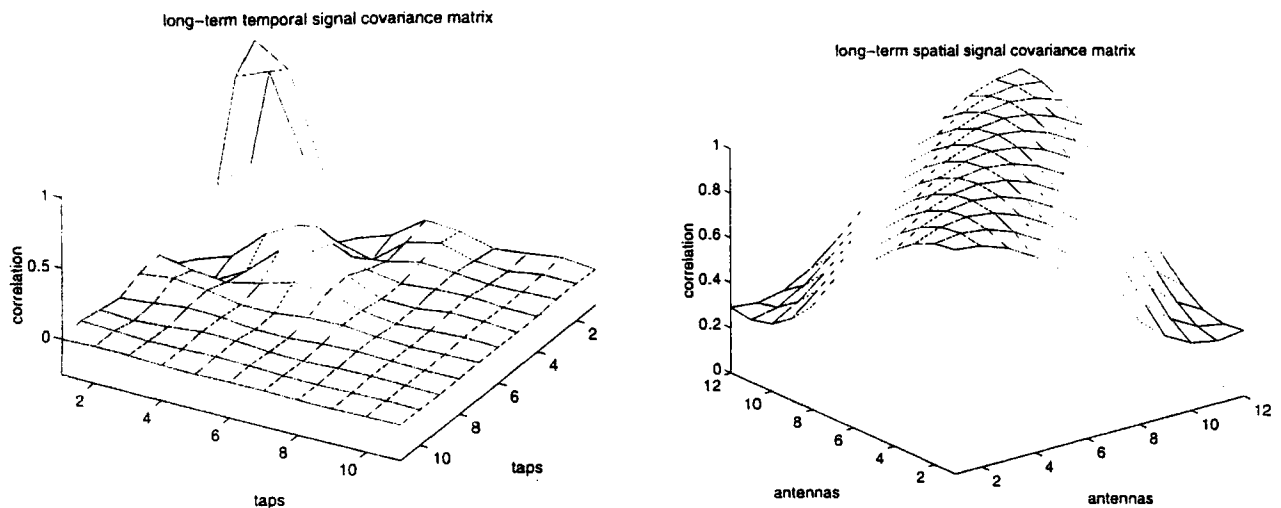


Figure 1: Structure of a long-term temporal for a picocellular environment with an oversampling factor of $M_c = 2$ (left) and a long-term spatial signal covariance matrix for a frequency flat scenario with an angular spread of 70° received with a ULA with $M = 12$ antenna elements (right).

searcher selects the eigenvectors belonging to the dominant eigenvalues which serve as spatial filters. Thus, similarly to selecting dominant temporal taps whilst neglecting others, the spatial dimension is reduced from the number of antenna elements to the number of selected eigenvalues⁶.

The spatial eigenrake can easily be extended to frequency selective channels. To this end, spatial processing as described above is performed for each dominant temporal tap. Recall that the temporal taps are uncorrelated due to the US-assumption and, therefore, the output of spatial filters which apply to different temporal taps (which are separated by at least one chip duration) are uncorrelated as well. In Figure 2, the long-term spatial eigenvalues of four temporal taps are plotted for a spatially selective scenario. Accordingly, the four largest eigenvalues belong to the first two temporal taps. Therefore, if the receiver is restricted to four rake fingers, in the present scenario these would be applied to the first two taps only by using the two corresponding eigenvectors for each tap as spatial filters. (In contrast, the beamformer rake would deploy one rake finger per temporal stage and use the dominant eigenvector of this temporal stage only.)

By taking into account the long-term spatio-temporal structure of the mobile radio channel, *short-term processing* is improved with respect to accuracy of the (compressed) spatio-temporal channel estimate and with respect to the computational complexity. In general, a significant reduction in dimension can be achieved depending on the long-term properties of the mobile radio channel.

⁶In other words, modelling the radio channel by its low-rank approximation.

3 UPLINK PROCESSING: EIGENRAKE

3.1 CHANNEL AND SIGNAL MODEL

We assume that the narrowband assumption holds. In this case, each wavefront arriving at different antenna elements can be characterized by a phase shift. Hence, the baseband representation of the $M \times 1$ array snapshot vector $\mathbf{x}(t)$ containing the outputs of each of the M antenna elements after the channel filter at time t is modeled as

$$\begin{aligned} \mathbf{x}(t) = & \sum_{i=1}^L \xi_i \mathbf{a}(\mu_i) s(t - \tau_i) * p(t) \\ & + \sum_{k=2}^K \sum_{i=1}^{L_k} \xi_i^{(k)} \mathbf{a}^{(k)}(\mu_i) s^{(k)}(t - \tau_i^{(k)}) * p(t) \\ & + \mathbf{n}(t), \end{aligned} \tag{5}$$

where $\mathbf{a}(\mu_i)$, τ_i , and ξ_i denote the steering vector, the delay, and the complex amplitude of each wavefront, respectively. Furthermore, L is the number of impinging wavefronts and the convolution operator is denoted by $*$. The subscript i denotes the wavefront and the index k denotes the user. We have omitted the index $k = 1$ for the parameters of the user of interest. For instance, the steering vector of the i -th wavefront would correspond to

$$\mathbf{a}(\mu_i) = [1 \quad e^{j\mu_i} \quad \dots \quad e^{j(M-1)\mu_i}]^T$$

in case of a uniform linear array (ULA) with omnidirectional antenna elements. Here $\mu_i = \omega \frac{\Delta}{c}$ where ω , Δ , and c denote the frequency, the antenna element spacing, and the speed of light, respectively.

In the uplink, data and control channel are mapped to the I and Q branches and the baseband signal corresponds

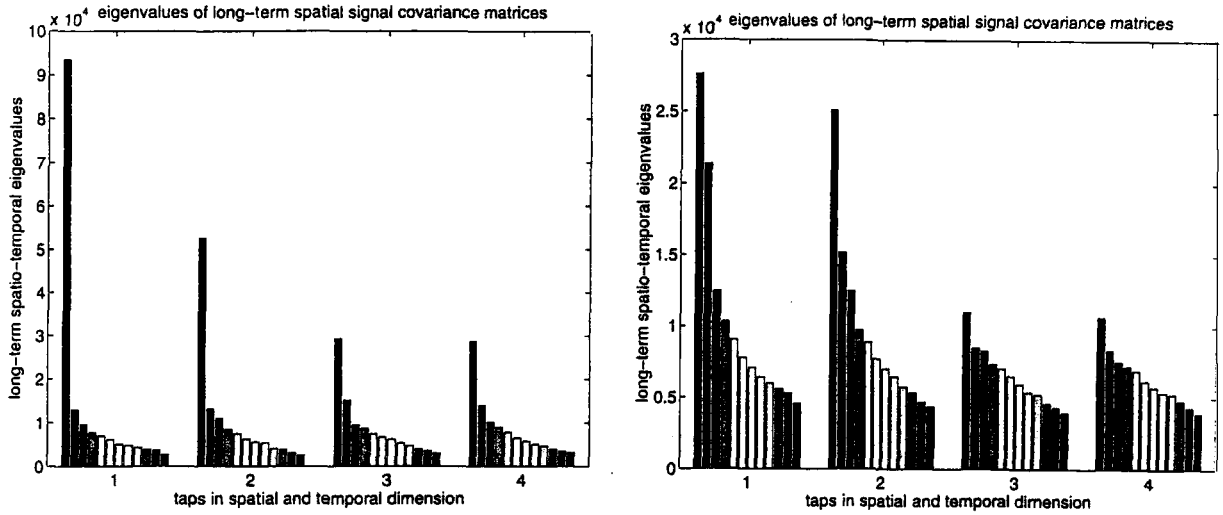


Figure 2: The left plot shows long-term spatial eigenvalues of 4 temporal taps for a spatially non-selective scenario (rural). On the right, the long-term eigenspectra is plotted for a spatially selective scenario (picocellular) for 4 temporal taps.

to

$$s(t) = \beta \cdot s_D(t) + j \cdot s_C(t), \quad (6)$$

where β denotes the power of the DPDCH⁷ in relation to the DPCCCH⁸. Moreover, W-CDMA uses a chip waveform, $p(t)$, characterized by a square-root raised cosine spectrum with a rolloff factor of $\alpha = 0.22$. Accordingly, the baseband signal of a data channel equals

$$s_D(t) = \sum_{\ell=-\infty}^{\infty} b_D^{(\ell)} z_D(t - \ell T_D), \quad (7)$$

$$z_D(t) = \sum_{q=1}^{Q_D} c_D^{(q)} p(t - qT_c), \quad (8)$$

where the chip rate is $1/T_c = 3.84$ Mchips/s. Moreover, the spreading code of the DPDCH, $z_D(t)$, is of length $T_D = Q_D T_c$ and is composed of Q_D chips $c_D^{(q)} \in \{-1, 1\}$, $1 \leq q \leq Q_D$. The carrier is modulated by BPSK symbols, namely $b_D^{(\ell)} \in \{-1, 1\}$.

3.2 EIGENRAKE

The structure of the space-time eigenrake resulting from the dimension reduction concept described in Section 2 is depicted in Figure 3. In notational terms, the overall procedure can be put in the following form. We construct a spatial compression matrix from the spatial filters selected by the space-time rake searcher according to

$$C^{(S)} = \begin{bmatrix} w_1^{(S)} & w_2^{(S)} & \dots & w_{N_f}^{(S)} \end{bmatrix} \in \mathbb{C}^{M \times N_f}. \quad (9)$$

⁷Dedicated Physical Data Channel.

⁸Dedicated Physical Control Channel.

Likewise, we can construct a temporal compression matrix $C^{(T)} \in \mathbb{R}^{N_d \times N_f}$. All entries of n -th column of $C^{(T)}$ are "0"s, except for a single "1" at the position of the n -th temporal rake finger. This position is associated with a spatial filter and is determined by the space-time rake searcher. Then the compressed space-time vectors *before* and *after* the correlator are defined as

$$x_c^{(\ell)} = \text{diag} \left\{ C^{(S),H} \mathcal{X} J^{(\ell)} C^{(T)} \right\}, \quad (10)$$

$$h_c = \text{diag} \left\{ C^{(S),H} \mathcal{H} J^{(1)} C^{(T)} \right\}, \quad (11)$$

where the rows of the data matrices $\mathcal{X} \in \mathbb{C}^{M \times N}$ and $\mathcal{H} \in \mathbb{C}^{M \times N}$ contain the spatial snapshots $x(t)$ and $h(t)$ sampled at M_c times the chip rate $1/T_c$ *before* and *after* the (pilot) correlator, respectively. Moreover, a temporal selection matrix

$$J^{(\ell)} = \begin{bmatrix} 0_{(l-1) \times N_d} \\ I_{N_d \times N_d} \\ 0_{(N-l-N_d+1) \times N_d} \end{bmatrix}$$

is applied to the correlator output \mathcal{H} such that $\mathcal{H} J^{(1)} \in \mathbb{C}^{M \times N_d}$ contains all multipath components. The short-term compressed measurement covariance matrix equals

$$K_{X,c} = \text{mean} \left\{ x_c^{(\ell)} \cdot x_c^{(\ell),H} \right\}. \quad (12)$$

Note that l is limited to the spatial snapshots within the time coherence of the channel. Assuming that the channel stays approximately constant for at least one slot, the compressed space-time weight vector $w_c^{(ST)}$ can be found by solving $h_c = K_{X,c} w_c^{(ST)}$. Interference suppression in the short term supports interference suppression in the long term especially if, for instance, eigenbeams belonging to

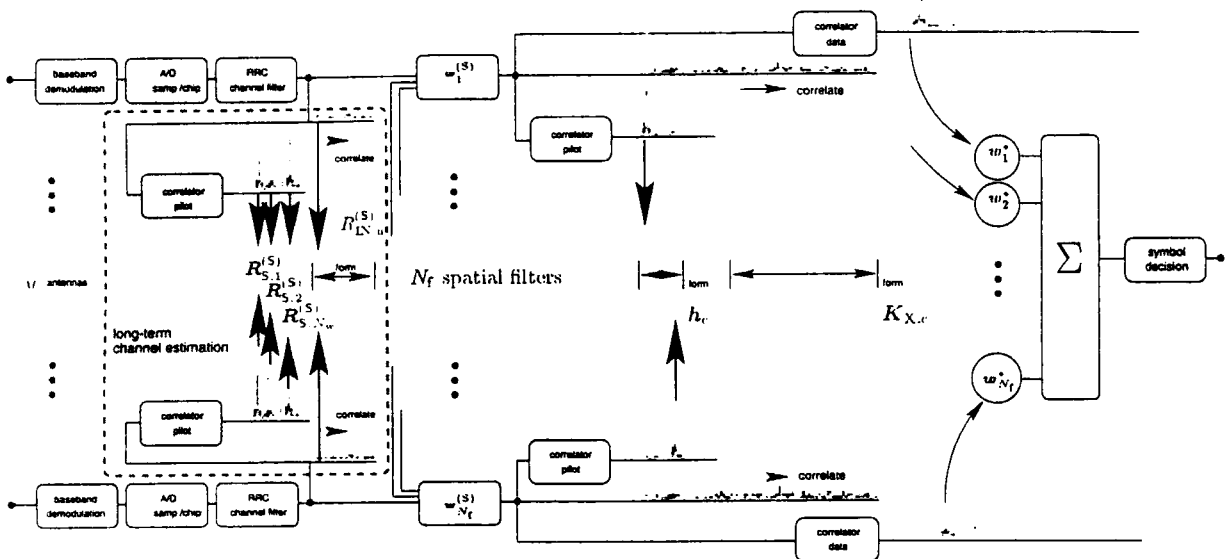


Figure 3: Structure of the space-time eigenrake.

different temporal taps are based on wavefronts with similar directions of arrival. In this case, short-term temporal correlations are exploited to reduce interference.

In real systems, the WSS assumption does not hold. Therefore, we use a forgetting factor ρ which, in the example below, is applied to the long-term spatial signal covariance matrix of the n -th tap

$$\mathbf{R}_n^{(S)} \leftarrow \rho \mathbf{R}_n^{(S)} + (1 - \rho) \mathbf{h}_n^{(S)} \mathbf{h}_n^{(S),H} \in \mathbb{C}^{M \times M}. \quad (13)$$

Typically, the forgetting factor lies between $0.99 \leq \rho \leq 0.999$ depending on the scenario (velocity and positions of users, scatterers, and base). Accordingly, long-term processing can be spread over many slots since the update described in (13) has to be done only once per frame (=15 slots) or even less frequently and, therefore, is computationally not complex. Note that the eigenrake corresponds to a decoupled space-time rake for $\rho = 0$. Notice, moreover, that for a small ρ or for a slowly changing channel, long-term and short-term channel properties are mixed within \mathbf{R}_n .

3.3 SIMULATION RESULTS

Our performance measure is the raw bit error ratio (BER) of data channel (DPDCH) symbols. Voice service with a spreading factor of $Q_D = 128$ in the data channel has a correlation gain of 21 dB and is supposed to be only 3 dB above the noise and interference level after correlation. This is sufficient for a raw BER lower than 10% using BPSK [27]. A raw BER of approximately 10% is required to ensure a sufficient BER after decoding for voice service in the uplink of W-CDMA. Moreover, power control is performed slotwise. For simplicity, power control is not based on the output SINR at the mobile receivers but on the received signal power at each antenna element.

Adaption is performed exactly instead of taking place in steps of, for instance, 1 dB. In the simulations based on the rural environment, we assumed a service mix of 1:2.5 between strong high data-rate interferers and weak voice interferers which have a spreading factor in the data channel of $Q_D = 8$ and $Q_D = 128$, respectively. To compensate for the correlation gains, the power of the data channel of the high data-rate interferers is received 16 times the power of the data channel of the voice interferers. The spreading factor in the control channel equals $Q_C = 256$ and $N_P = 6$ pilot symbols per slot are provided for channel estimation. Further simulation parameters are chosen as follows. We used a uniform linear array (ULA) with omnidirectional antenna elements and an antenna distance of $\Delta = 0.5\lambda_c$ where λ_c denotes the carrier wavelength and an oversampling factor of $M_c = 2$. The user of interest is characterized by $\beta = 2$, cf. (6), and $Q_D = 128$. The forgetting factor used to average the long-term spatial covariance matrices required by the beamformer rake and the ST eigenrake is set to $\rho = 0.999$, cf. (13). Recall that the closer the forgetting factor approaches 1, the less computational complexity is involved in long-term processing since the long-term processing steps can be spread over many frames. To reduce simulation time, the weak voice interferers are modeled as spatially and temporally white noise which is passed through a channel filter before it is added to the channel.

Let us continue with a list of the receiver structures which are compared: MRC ST rake, joint space-time rake, beamformer rake, and space-time eigenrake. We have modified the MRC space-time rake to consider only the dominant temporal taps. The simulation time equals 500 ms, the channel estimate is performed using the pilot sequence of the current slot, and $N_f = 3$ rake fingers are selected⁹.

⁹The MRC ST rake generates as many diversity branches as antenna

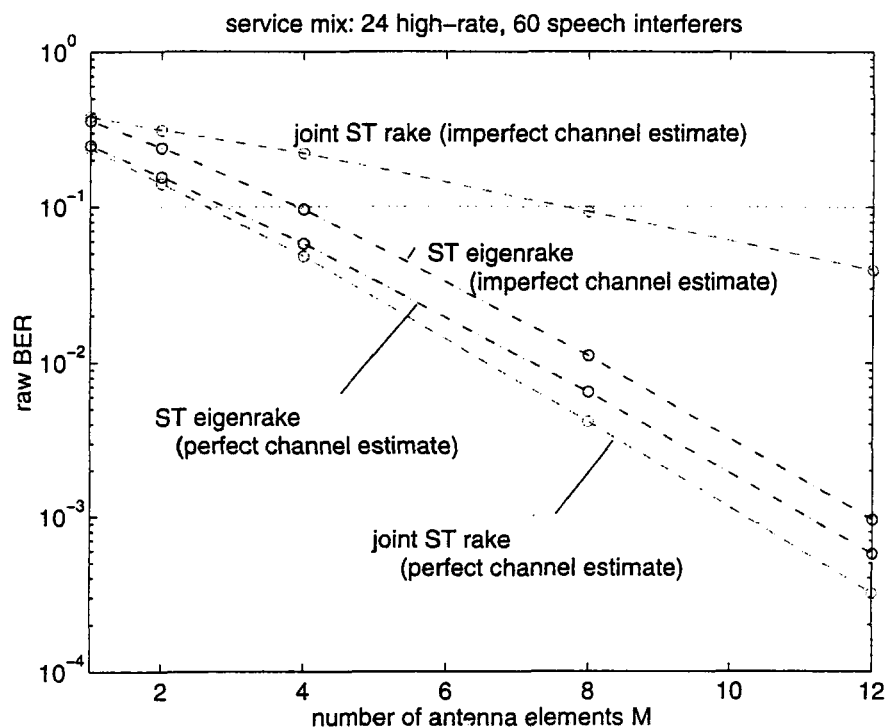


Figure 4: Rural environment: The interference is characterized by 24 strong and 60 weak users. We compare the performance of the space-time eigenrake and the joint space-time rake for a perfect channel estimate and a channel estimate obtained with the pilot sequence of the current slot.

In Figure 4, we compare the performance of the space-time eigenrake and the joint space-time rake for a perfect channel estimate and a channel estimate using the pilot sequence of the current slot. The performance of these schemes is lower bounded by the joint space-time rake using a perfect channel estimate. In this case, the degrees of freedom are used as efficiently as possible. The eigenrake using a perfect channel estimate performs only slightly worse. However, the distance with respect to the performance of the joint space-time rake with perfect channel estimates increases with an increasing number of antenna elements since the dimension of short-term processing within the eigenrake stays constant at N_f due to a fixed number of N_f spatio-temporal rake fingers. Note that the eigenrake using the channel estimate obtained with the pilot sequence of the current slot performs only slightly worse than the receiver structures with a perfect channel estimate. This means that the long-term processing of the eigenrake is able to improve the reduced-dimension short-term channel estimate considerably. Moreover, the performance of the eigenrakes with and without perfect channel estimate converges since the channel estimate based on one slot improves with increasing antenna gain. Finally, the joint space-time rake using the channel estimate based on the pilot sequence of the current slot performs considerably

elements times temporal rake fingers, $M \cdot N_f$, whereas beamformer and eigenrake limit the number of branches to the number of rake fingers N_f .

worse than any of the other receivers.

Figure 5 presents different rake receiver structures both in a rural environment and in a pico environment. Whereas the radio channel of a rural scenario is characterized by high spatial correlations, the spatial correlations in pico scenarios is low¹⁰. Consequently, in case of high spatial correlations (rural scenario) the ST eigenrake and beamformer rake perform similar since the eigenvectors chosen are the same¹¹. The MRC ST rake and joint ST rake fail due to their erroneous channel estimates which are the consequence of the excessive number of parameters. Otherwise, in case of low spatial correlations (pico scenario), now the ST eigenrake and MRC ST rake have similar performance since the eigenrake is capable to exploit more than one eigenvector per temporal tap. Accordingly, the beamformer rake degrades. Here, the case $M = 1$ in Figure 5 denotes the reference case of using one antenna element.

¹⁰The spatial selectivity of both types of radio channels behaves vice versa.

¹¹The ST eigenrake slightly shows better results due to optimum short-term processing – optimum combining instead of MRC.

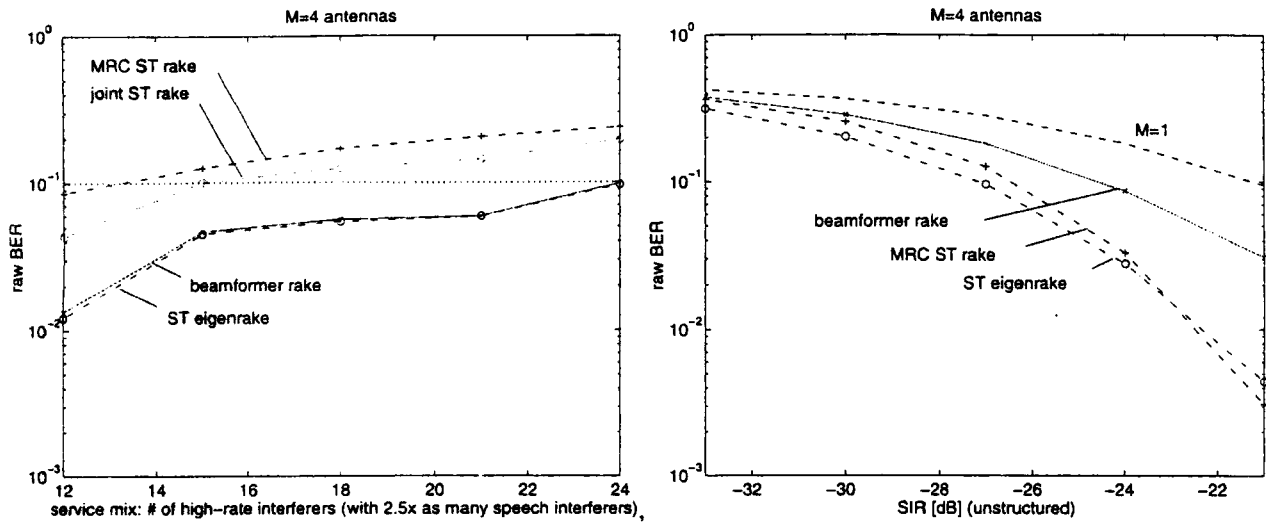


Figure 5: top: simulation results rural ($N_t = 3$), down: simulation results picocellular ($N_t = 4$)

4 DOWNLINK PROCESSING: DOWNLINK EIGENBEAMFORMER

4.1 CHANNEL AND SIGNAL MODEL

The baseband representation of the scalar snapshot value $x(t)$ at the mobile containing the weighted sum of transmit signals from the M antenna elements at the BS after the channel filter is modelled as

$$x(t) = \sum_{n=1}^{N_t} \mathbf{w}^{(S),H} \mathbf{h}_n^{(S)} s(t - \tau_n), \quad (14)$$

where $\mathbf{h}_n^{(S)}$, $\mathbf{w}^{(S),H}$, and τ_n denote the short-term spatial channel impulse response, the selected eigenbeam, and the delay of the n -th tap. Furthermore, N_t equals the number of dominant temporal channel taps, i.e. in (14) a dimension reduction in terms of temporal channel taps has already taken place.

Moreover, the spatial channel impulse response for the n -th tap $\mathbf{h}_n^{(S)}$ can be modelled according to [29, 30]

$$\mathbf{h}_n^{(S)} = \mathbf{R}_{X,n}^{(S),\frac{1}{2}} \mathbf{g}_n(t). \quad (15)$$

To this end, $\mathbf{R}_{X,n}^{(S),\frac{1}{2}}$ denotes the Cholesky decomposition of the long-term spatial correlation matrix $\mathbf{R}_{X,n}^{(S)}$ which contains the correlations between antennas for the n -th tap, and the vector $\mathbf{g}_n(t)$ describes a normalized zero-mean Gaussian fading process with Jakes power density spectrum, cf. [31].

In the downlink, the DPDCH and DPCCH are time-multiplexed instead of code-multiplexed as in the uplink. In addition to user dedicated pilot symbols which are optionally transmitted within the DPCCH to enable an accurate channel estimation if adaptive antennas and downlink beamforming schemes are employed, an omnidirectional

pilot channel is broadcasted in the downlink. To enable spatial downlink channel estimation, e.g. $\mathbf{h}_n^{(S)}$ and $\mathbf{R}_{X,n}^{(S)}$, at the mobile, orthogonal pilot sequences must be transmitted from each antenna element at the BS if an antenna array is available at the BS. Orthogonal pilot sequences for two antenna elements are defined in the current W-CDMA standard.

For the sake of notational simplicity, we assume that the power and spreading codes are identical for the DPDCH and the DPCCH of each mobile, i.e., $Q = Q_d = Q_c$ holds. Again, scrambling is not included in the notation. Then the downlink baseband signal in the dedicated physical channel corresponds to

$$s^{env}(t) = \sum_{\ell=-\infty}^{\infty} b^{(\ell)} z(t - \ell T), \quad (16)$$

$$z(t) = \sum_{q=1}^Q c^{(q)} p(t - qT_c). \quad (17)$$

The spreading code, $z(t)$, is of length $T = QT_c$ and is composed of Q chips $c^{(q)} \in \{-1, 1\}$, $1 \leq q \leq Q$. The carrier is modulated by QPSK symbols, namely $b^{(\ell)} \in \{1, j, -1, -j\}$. Notice that downlink transmission is synchronized on the symbol level to exploit the orthogonality of the OVFS codes which are used as spreading codes¹².

4.2 DOWNLINK EIGENBEAMFORMER

The general idea behind the downlink eigenbeamformer is a decorrelation of (spatial) diversity branches to achieve a reduction in dimension for subsequent short-term processing and an improved short-term channel estimate at

¹²There are severe restrictions to which OVFS codes can be used in the downlink since separation is achieved by the spreading codes and not by the scrambling codes as on the uplink.

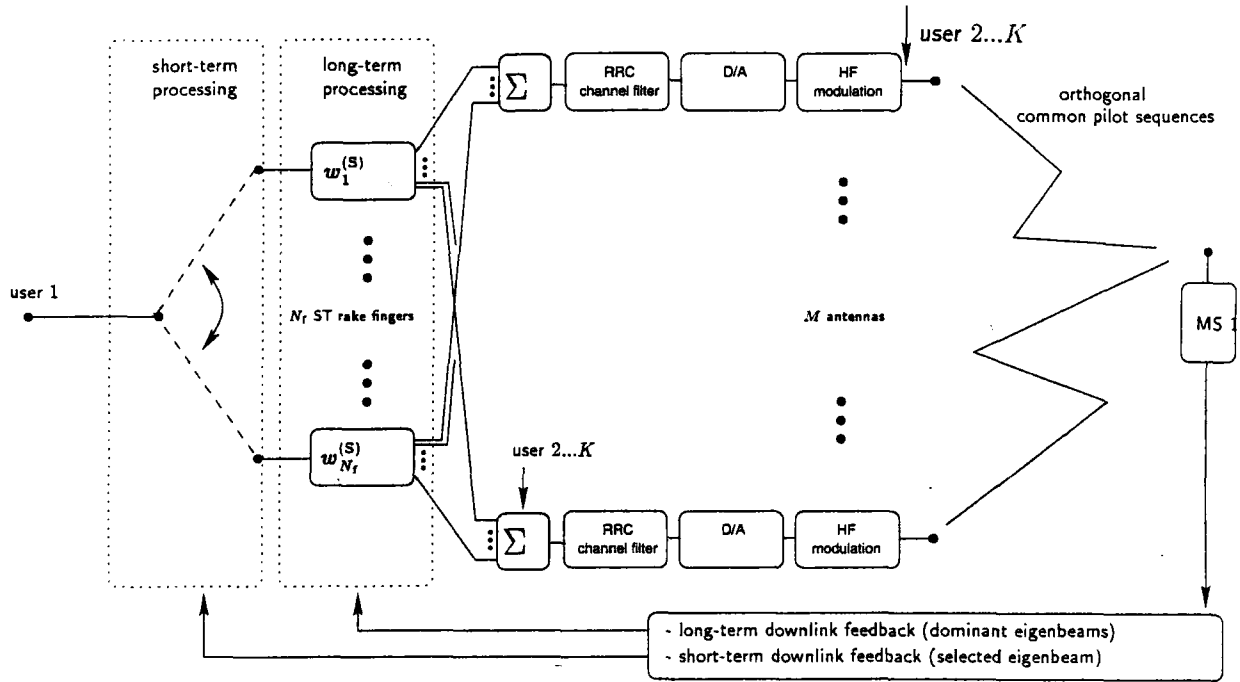


Figure 6: Structure of the downlink eigenbeamformer using long-term and short-term feedback.

the mobile terminal enabled by an increase in diversity and antenna gain and interference suppression. To this end, the *eigenvectors or eigenbeams* of the long-term spatial covariance matrices with the largest eigenvalues (largest average SNR) are determined and fed back step by step to the base station. This process takes place on the same time scale as the physical terminal movement. Accordingly, required operations at the mobile terminal as well as required feedback bits are distributed over a very large number of slots. In addition, a short-term selection between the eigenbeams is carried out at the terminal to account for fast fading and is fed back. Thus, one is able to efficiently address a large number of M antenna elements by having the terminal select one out of a reduced set of N_r eigenbeams, cf. reduction in dimension, and feed back this information to the BS. In other words, the downlink eigenbeamformer resembles a switching diversity concept on top of the low-rank approximated radio channel. The structure of the downlink eigenbeamformer is depicted in Figure 6.

It has been demonstrated that the downlink eigenbeamformer is a valuable candidate to outperform competing closed-loop Tx diversity concepts both in macro cell and micro cell environments [32, 33].

The computation of the dominant eigenvectors $w_d^{(S)} \in \mathbb{C}^M$ comprises the estimation and the PCA of the long-term spatial covariance matrix $R_X^{(S)}$:

$$R_X^{(S)} = W^{(S)} \Lambda W^{(S),H}, \quad (18)$$

where $W^{(S)} = [w_1^{(S)} \ w_2^{(S)} \ \dots \ w_M^{(S)}] \in \mathbb{C}^{M \times M}$ and $\Lambda = \text{diag}[\lambda_1 \ \lambda_2 \ \dots \ \lambda_M] \in \mathbb{C}^{M \times M}$ denote the matrices of eigenvectors and eigenvalues, respectively.

At first, the estimation of long-term spatial covariance matrices (second order statistics) requires orthogonal pilot sequences transmitted from each BS antenna element. Since the second order statistics of the signals change slowly over time, a forgetting factor ρ is used which, in the example below, is applied to the long-term spatial signal covariance matrix as follows:

$$R_X^{(S)} \leftarrow \rho R_X^{(S)} + (1 - \rho) \sum_{n=1}^{N_d} h_n^{(S)} h_n^{(S),H} \in \mathbb{C}^{M \times M}. \quad (19)$$

In contrast to (13), the long-term spatial covariance matrices of the dominant temporal taps are averaged before the decomposition. This is required since a signal transmitted at the base station in general affects more than one temporal tap at the mobile terminal receiver¹³.

¹³The vector $w_d^{(S)}$ aims at maximizing the accumulated ratios $\sum_n \frac{w_d^{(S),H} R_{X,n}^{(S)} w_d^{(S)}}{w_d^{(S),H} w_d^{(S)}} = \frac{w_d^{(S),H} \sum_n R_{X,n}^{(S)} w_d^{(S)}}{\|w_d^{(S)}\|^2}$ which are related to the transmitted power from the BS to the mobile.

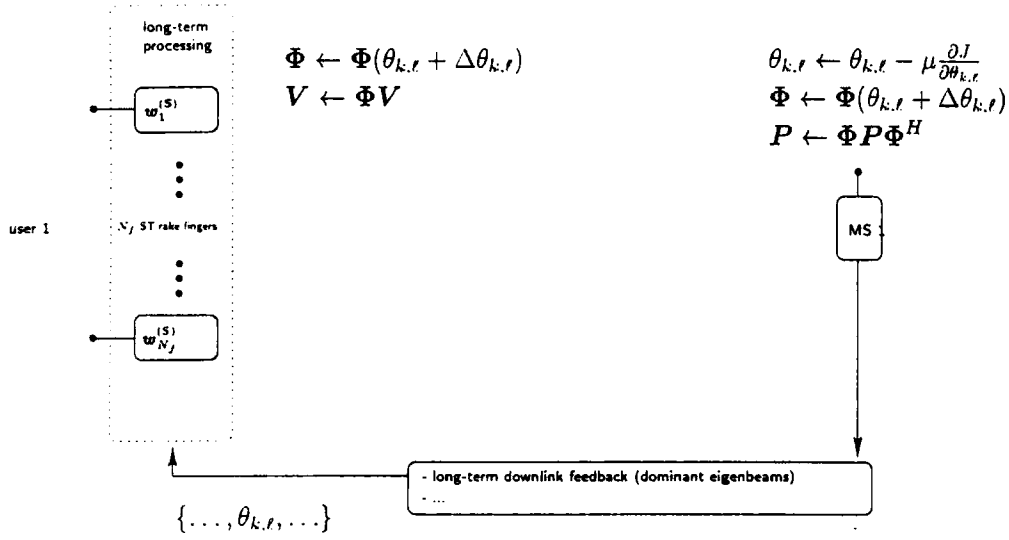


Figure 7: Illustration of the distributed implementation of the eigenspace tracking.

4.3 SUBSPACE TRACKING FOR DOWNLINK EIGEN-BEAMFORMER

Even if the rate of updating the long-term estimates of channel properties is not demanding, the efficiency of any closed-loop Tx diversity concept depends on two vital items: (i) the amount of required feedback information per time and (ii) computational and numerical effort spent at the mobile terminal. To this end, we deploy a recently proposed subspace tracking technique [34] for tracking the eigenbeams which accomplishes both requirements.

The new tracking algorithm resumes the tradition of estimating subspaces by the solution of an unconstrained optimization problem [35, 36]. Resuming the ideas of [36], it has been shown in [34] that the objective function

$$\begin{aligned}
 J(\Phi) &\triangleq -E \left[\mathbf{x}^H \Phi P \Phi^H \mathbf{x} \right] \\
 &= -\text{tr} \left[\mathbf{W}_o^{(S),H} \Phi^H E \left[\mathbf{x} \mathbf{x}^H \right] \Phi \mathbf{W}_o^{(S)} \right] \\
 &= -\text{tr} \left[\mathbf{V}^H \mathbf{R}_X^{(S)} \mathbf{V} \right], \quad (20)
 \end{aligned}$$

with the projection matrix $P = \mathbf{W}_o^{(S)} \mathbf{W}_o^{(S),H} \in \mathbb{C}^{M \times M}$ and $\mathbf{V} = \Phi \mathbf{W}_o^{(S)} \in \mathbb{C}^{M \times d}$, attains its global minimum at Φ^* if and only if

$$\mathbf{V}^* = \Phi^* \mathbf{W}_o^{(S)} = \mathbf{W}_{N_f}^{(S)} \Psi, \quad (21)$$

where $\mathbf{W}_{N_f}^{(S)}$ is the matrix of the eigenvectors of the N_f largest eigenvalues of $\mathbf{R}_X^{(S)}$. Here, the matrices $\Phi \in \mathbb{C}^{M \times M}$ and $\Psi \in \mathbb{C}^{N_f \times N_f}$ are unitary rotation matrices.

It turns out that the iterative minimization of $J(\Phi)$ considerably benefits from an alternative parameterization of Φ . To this end, Φ is denoted as the product of elementary rotation matrices¹⁴, (cf. 22), where $k = M - 1, \dots, 1$ and

¹⁴In the case of $M = 4$ antenna elements, the parameterization of the unitary rotation matrix reads $\Phi_{4 \times 4} = \Gamma \cdot \Phi^{3,4} \cdot \Phi^{2,3} \cdot \Phi^{2,4} \cdot \Phi^{1,2} \cdot \Phi^{1,3} \cdot \Phi^{1,4}$.

$\ell = k + 1, \dots, M$.

The $\Phi^{k,\ell}$ are Givens rotation matrices with the characteristic entries at (k, k) , (k, ℓ) , (ℓ, k) , and (ℓ, ℓ) , i.e. the defining submatrix, the Givens rotor $\mathbf{G}^{k,\ell} \in \mathbb{R}^{2 \times 2}$, is equal to

$$\mathbf{G}^{k,\ell} \triangleq \begin{bmatrix} +\cos(\theta_{k,\ell}) & -\sin(\theta_{k,\ell}) \\ +\sin(\theta_{k,\ell}) & +\cos(\theta_{k,\ell}) \end{bmatrix}. \quad (23)$$

The rescaling matrix Γ is given by

$$\Gamma \triangleq \text{diag} \left[e^{j\theta_1}, e^{j\theta_2}, \dots, e^{j\theta_M} \right]. \quad (24)$$

Hereby, the parameterization of Φ and thus, regardless of the dimension N_f , the parameterization of $\text{span} \left[\mathbf{W}_{N_f}^{(S)} \right]$ which equals the subspace of dominant eigenbeams requires $\frac{M(M+1)}{2}$ elements. Note, that all θ are real-valued and only take values from $[-\pi, +\pi[$ and $[-\frac{\pi}{2}, +\frac{\pi}{2}[$ ¹⁵.

Obviously, the tracking of the dominant eigenbeams is closely related to the tracking of the parameters θ :

$$\theta \leftarrow \theta - \mu \frac{\partial J}{\partial \theta}, \quad (25)$$

where the $\frac{\partial J}{\partial \theta}$ constitute the gradient of J . It has been shown that the partial differentials can be obtained as a rather straightforward function¹⁶ of P and $\mathbf{R}_X^{(S)}$.

¹⁵For more readability the indices of $\theta_{k,\ell}$ and θ_k are generally omitted.

¹⁶Given the objective function

$$J(\Phi(\theta)) \triangleq -\text{tr} \left[\mathbf{W}_{N_f}^{(S),H} \Phi(\theta)^H \mathbf{R}_X^{(S)} \Phi(\theta) \mathbf{W}_{N_f}^{(S)} \right],$$

it has been shown that.

- in the case of $k \neq \ell$, the partial differentials of J can be derived by

$$\frac{\partial J}{\partial \theta_{k,\ell}} = 2 \left(\text{Real} \left[\mathbf{V}^{(l)} \Upsilon_{(k)} \right] - \text{Real} \left[\mathbf{V}^{(k)} \Upsilon_{(l)} \right] \right),$$

- whereas in the case of $k = \ell$

$$\frac{\partial J}{\partial \theta_{k,k}} = 2 \left(\text{Imag} \left[\mathbf{V}^{(k)} \Upsilon_{(k)} \right] \right).$$

$$\Phi \triangleq \Gamma \cdot \Phi^{M-1, M} \cdot \Phi^{M-2, M-1} \cdot \Phi^{M-2, M} \dots \Phi^{k, \ell} \dots \Phi^{1, M-1} \cdot \Phi^{1, M}, \quad (22)$$

Consequently, for all θ the update of the matrices Φ , V , and P are equal to

$$\Phi \leftarrow \Phi(\theta + \Delta\theta), \quad (26)$$

$$V \leftarrow \Phi V, \quad (27)$$

$$P \leftarrow \Phi P \Phi^H, \quad (28)$$

respectively. In spite of the complex nature of the algorithm, the total update of one iteration cycle requires only $3M^2N_f$ complex multiplications¹⁷, i.e. considering a 4-antenna-Tx concept and $N_f = 2$ it takes 96 complex multiplications to compute one update cycle.

Although the column vectors v of the matrix V constitute the eigenspace of the dominant eigenbeams, the vectors V are not fully decorrelated. Therefore, if perfect decorrelation of channels is a must, a further decorrelation step by means of the unitary rotation matrix Ψ is performed by

$$W_{N_f}^{(S)} \leftarrow V \Psi^H \quad (29)$$

which directly results from (21). The matrix Ψ again can be parameterized and estimated very likely as Φ , however at the lower dimension $N_f < M$. Consequently, in the sequel we distinguish between parameters θ_Φ and θ_Ψ .

Note, that $J(\Phi)$ is invariant to short-term fluctuations of the estimates of $R_X^{(S)}$. Accordingly, the proposed scheme of separating the eigenbeam tracking in rotations of Φ and Ψ allows to reduce the forgetting factor ρ without giving up the access to the long-term characteristics of the channel.

Long/Short-Term Feedback

The nature of the proposed eigenbeam tracking algorithms ditto offers an alternative concept for the feedback of the eigenbeams from the mobile to BS. To this end, instead of directly communicating the eigenvectors via the closed-loop feedback channel, we propose to transmit the increments of the parameters θ .

The general idea behind this feedback concept is based on a *distributed implementation* of the eigenspace/-beam tracking, cf. Figure 7. Accordingly, the tracking of the parameters θ_Φ (25) and θ_Ψ is iteratively performed at the mobile, however the tracking of the eigenspace V (27) and the eigenbeams $W_{N_f}^{(S)}$ (29), respectively, is accomplished

Here, the $V^{(k)}$ and $Y_{(l)}$ denote the k -th row-vector and the l -th column vector of the matrices V and Y , where the latter is defined as $Y = V^H R_X^{(S)}$. Note, that the partial differentials are taken at $\theta_{k, \ell} = 0$ and $\theta_k = 0$, respectively.

¹⁷Computation of Y and the gradient, and updating the projection matrix (28) requires M^2N_f , $M(M-1)N_f + MN_f$, and $M(M-1)N_f + MN_f$ complex multiplications, respectively. For DSP implementations of the proposed method we refer to [37, 38].

at the BS¹⁸. Hereby, the size of the feedback signalling is solely determined by the number of parameters according to Φ , i.e. $\frac{M(M+1)}{2}$ incremental rotation angles¹⁹.

The proposed feedback signalling would offer a number of beneficial factors:

- The numerical complexity of the tracking algorithm is lower or equal than for standard techniques [38].
- The amount of feedback signalling is independent of the number of dominant eigenbeams N_f , cf. Table 1.
- The choice between updating Φ and Ψ enables to differentiate between estimation of long-term and short-term properties of the spatially correlated fading channel.
- Although the increase of required parameters grows quadratic with the number of antenna elements instead of the linear increase with standard feedback of eigenvectors, the size of feedback signalling for realistic implementations is even lower, cf. Table 1.
- Since the proposed subspace tracking algorithm converges very rapidly to the true eigenspace, the initialization of eigenbeams at the BS is not required [34].
- The subspace tracking algorithm is more robust against erroneous feedback information, cf. 8.
- The feedback format is compatible to the parameterization aligned to CORDIC²⁰ based processor arrays, and is thus highly suitable for VLSI implementations of the tracker at the mobile and the BS.

4.4 SIMULATION RESULTS

The proposed performance measure is given by the ratio of the power for the user of interest and the total Tx power of the relevant base station which is required to obtain a certain raw bit error ratio for the user of interest. Basically, the simulation environment compares to that used in [39]. Figure 8 presents the proposed performance measure for different velocities of the mobile²¹: 3, 10, 40, and 120 km/h. The downlink eigenbeamforming is either based on

¹⁸In addition to maintain the tracking algorithm at the mobile the tracking of the projector matrix (28) is performed at the BS.

¹⁹Note, in order to constrain the feedback effort the parameters θ_Φ and θ_Ψ are transmitted from mobile to BS in a rotatory modus without degradation of the estimation.

²⁰COordinate Rotation on a DIgital Computer.

²¹Note that variations in performance as a function of the velocity also depend on the power control. Here, power control is optimized for a target SINR at the rake receiver output which not necessarily maximizes mean raw BER for a low mean transmit power.

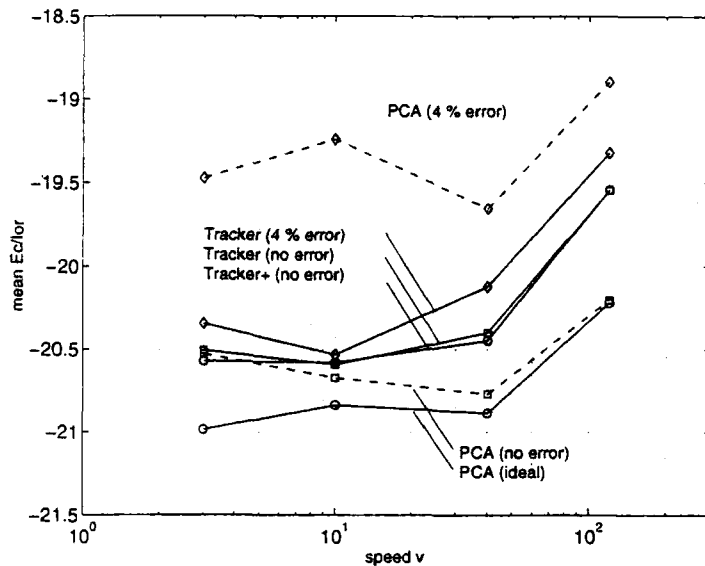


Figure 8: Performance of closed-loop downlink eigenbeamforming based on the standard PCA method and the subspace tracking method for the forgetting factor $\rho = 0.99$. The results are based on simulating data transmission while the mobile moves 30 seconds parallel to the BS antenna array.

- a standard PCA²²
- the proposed eigenbeam tracking algorithm²³ with a forgetting factor of $\rho = 0.99$.

In both cases a quantization of 4 bits per real/imaginary feedback quantity has been applied. The channel model was chosen according to [29] and the parameters are defined in [30, 40]. Consequently, the time delay between the mobile and the BS is due to the constrained feedback rate of 1500 Hz, i.e. for the use of $N_f = 2$ eigenbeams the feedback of a complete update of the eigenspace requires 810 slots for the case of the PCA solution and 600 slots for the tracking algorithm.

The simulated performance demonstrates the higher robustness of the tracking solution against the PCA in the case of erroneous feedback – the assumed error probability of the binary symmetric feedback channel is 4 %.

5 CONCLUDING REMARKS

The eigenbeamforming concept achieves reduced dimension processing by exploiting long-term channel properties and obtains decorrelated diversity branches in space and time by performing eigenvalue decompositions of the spatial covariance matrices of the dominant temporal taps (uplink) or of the mean of the spatial covariance matrices

²²Note, that in all cases the PCA has been calculated by available state-of-the-art linear algebra tools without considering the implied numerical imperfections of real applicable algorithms. Thus, in contrast as with the proposed eigenspace tracker the PCA results are rather overoptimistic.

²³The tracking has been applied with (Tracker+) and without (Tracker) the decorrelation step, cf. (29).

Table 1: The number of required bits for $M = 4, 6,$ and 8 antenna elements to transmit $d = 2$ or 3 eigenbeams from the mobile to the BS by means of 4 bits per parameter increment θ . The numbers in (·) the number of required bits to feedback the eigenvectors by means of 4 bits per real/imaginary part of a vector element.

M	$d = 2$		$d = 3$	
4	40	(64) bits	40	(96) bits
6	84	(96) bits	84	(144) bits
8	144	(128) bits	144	(192) bits

(downlink). Based on the eigenbeamforming concept, we have proposed a novel space-time receiver and transmitter structure for CDMA systems with adaptive antennas at the BS.

A novel rake receiver structure, namely the *space-time eigenrake* combines the advantages and eliminates the drawbacks of long-term beamforming and short-term optimum combining which characterize previously introduced rake receivers. The space-time eigenrake is based on decorrelating diversity branches to achieve a reduction in dimension or model order for subsequent short-term processing. Decorrelation and interference suppression is achieved by an eigenanalysis of the long-term channel properties. It has been demonstrated that, despite low computational complexity, the new structure outperforms previously known concepts. Another major advantage is that the eigenrake automatically adjusts to various propagation environments, whereas known concepts are typically well-suited only for

some scenarios but less so for others. Notice, furthermore, that additional diversity branches such as branches obtained by exploiting polarization can be integrated easily.

It is of great economic importance to have downlink processing schemes which exploit the mobile radio channel efficiently within the W-CDMA standard in order to maximize spectral efficiency. To this end, we have extended the general idea of eigenbeamforming to closed-loop diversity schemes on the downlink currently discussed in W-CDMA standardization bodies. With the *downlink eigenbeamformer* based on feedback, an increased diversity order and more interference suppression can be achieved by increasing the number of antenna elements without having to increase the feedback required for short-term processing.

Finally, we have presented a tracking solution to the downlink eigenbeamformer concept. In spite of the complex nature of the algorithm it offers a straightforward implementation with low complexity and a number of benefits for the feedback signalling. The reliability of the downlink eigenbeam tracking has been approved by simulation results.

Manuscript received on June 1, 2001.

REFERENCES

- [1] W.C. Jakes. *Microwave Mobile Communication*. IEEE Press, Piscataway, NJ, 1994. second ed.
- [2] J. Zhang, E.K.P. Chong, and I. Kontoyiannis. Unified spatial diversity combining and power allocation schemes for CDMA systems. In *Proc. IEEE GLOBECOM*, San Francisco, CA, November 2000.
- [3] *Third Generation Partnership Project (3GPP)*, 2000. www.3gpp.org.
- [4] J.H. Winters. Optimum combining in digital mobile radio with cochannel interference. *IEEE Journal on Selected Areas in Communications*, SAC-2, no. 4:528–539, July 1984.
- [5] X. Bernstein and A.M. Haimovich. Space-time optimum combining for CDMA communications. *Wireless Personal Communications*, 3:73–89, 1996. Kluwer Academic Publishers.
- [6] C. Brunner, M. Haardt, and J.A. Nossek. On space-time rake receiver structures for WCDMA. In *Proc. 33rd Asilomar Conf. on Signals, Systems, and Computers*, Pacific Grove, CA, October 1999.
- [7] C. Brunner. *Efficient Space-Time Processing Schemes for WCDMA*. Ph. D. dissertation, Munich University of Technology, Institute for Circuit Theory and Signal Processing, Munich, Germany, June 2000. ISBN 3-8265-8062-1.
- [8] S. Verdu. *Multiuser Detection*. Cambridge University Press, Cambridge, UK, 1998.
- [9] B.H. Khalaj, A. Paulraj, and T. Kailath. 2-D rake receivers for CDMA cellular systems. In *Proc. IEEE GLOBECOM*, pages 400–404, 1994.
- [10] A.F. Naguib. *Adaptive Antennas for CDMA Wireless Networks*. Ph. D. dissertation, Stanford University, Stanford, California, August 1996.
- [11] V.D. Van Veen and K.M. Buckley. Beamforming: A versatile approach to spatial filtering. *IEEE ASSP Magazine*, pages 4–24, April 1988.
- [12] J.C. Liberti and T.S. Rappaport. *Smart Antennas for Wireless Communications*. Prentice Hall, Upper Saddle River, New Jersey, 1st edition, 1999.
- [13] W. Utschick and F. Dietrich. Nonlinear receiver concepts in reduced dimension for WCDMA. 2001. *Submitted to GLOBECOM 2001, San Antonio*.
- [14] W. Utschick and F. Dietrich. Reduced dimension receiver concepts in the WCDMA uplink. In *Proceedings of the ITG-Diskussionsitzung 'Systeme mit intelligenten Antennen'*, 2001.
- [15] K.I. Pedersen, P.E. Mogensen, and F. Frederikson. Joint directional properties of uplink and downlink channel in mobile communications. In *Proc. 8th IEEE Int. Symp. on Personal, Indoor and Mobile Radio Commun. (PIMRC)*, Helsinki, Finland, September 1997.
- [16] *Third Generation Partnership Project (3GPP)*, 3G TS 25.214, 2000. www.3gpp.org.
- [17] M. Raitola, A. Hottinen, and R. Wichman. Transmission diversity in wideband CDMA. In *Proc. 49th IEEE Vehicular Technology Conf. Spring (VTC '99 Spring)*, pages 1545–1549, Houston, Texas, May 1999.
- [18] C. Brunner, J.S. Hammerschmidt, A. Seeger, and J.A. Nossek. Space-time eigenrake and downlink eigenbeamformer: Exploiting long-term and short-term channel properties in WCDMA. In *Proc. IEEE GLOBECOM*, San Francisco, CA, November 2000.
- [19] C. Brunner, J.S. Hammerschmidt, and J.A. Nossek. Downlink Eigenbeamforming in WCDMA. In *European Wireless 2000*, Dresden, Germany, September 2000.
- [20] Siemens. Advanced closed loop tx diversity concept (eigenbeamformer). TSG-R WG1 document, TSGR1#14(00)0853, Oulu, Finland, July 2000. www.3gpp.org.
- [21] W. Utschick and C. Brunner. Efficient tracking and feedback of DL-eigenbeams in WCDMA. In *Proceedings of the 4th European Personal Mobile Communications Conference, Vienna*, 2001.
- [22] C. Brunner, M. Haardt, and J.A. Nossek. Adaptive space-frequency rake receivers for WCDMA. In *Proc. IEEE Int. Conf. Acoust., Speech, Signal Processing*, Vol. 4, pages 2383–2386, Phoenix, Arizona, March 1999.
- [23] D.A. Pados and S.N. Batlana. Joint Space-Time Auxiliary-Vector Filtering for DS/CDMA Systems with Antenna Arrays. *IEEE Transactions on Communications*, 47(9), September 1999.
- [24] J.S. Goldstein, I.S. Reed, and L.L. Scharf. A Multistage Representation of the Wiener Filter Based on Orthogonal Projections. *IEEE Transactions on Information Theory*, 44(7):2943–2959, November 1998.

- [25] G.H. Golub and C.F. van Loan. *Matrix Computations*. Johns Hopkins University Press, Baltimore, MD, 3rd edition, 1996.
- [26] S. Anderson. *On Dimension Reduction in Sensor Array Signal Processing*. Ph. D. dissertation, Department of Electrical Engineering, Linköping University, Linköping, Sweden, 1992.
- [27] J.G. Proakis. *Digital Communications*. McGraw-Hill, New York, NY, 3rd edition, 1995.
- [28] P.A. Bello. Characterization of randomly time-variant linear channels. *IEEE Transactions on Communication Systems*, CS-11:360–393, December 1963.
- [29] Siemens. Channel model for tx diversity simulations using correlated antennas. Technical Report TSGR1#15 R1-00-1067, 3GPP TSG RAN WG 1, 2000.
- [30] Siemens. Simulation parameters for Tx diversity simulations using correlated antennas. Technical Report TSGR1#15 R1-00-1180, 3GPP TSG RAN WG 1, 2000.
- [31] J.S. Hammerschmidt. *Adaptive space and space-time processing for high-rate mobile data receivers*. Ph. D. dissertation, Munich University of Technology, Institute for Integrated Circuits, Munich, Germany, 2000.
- [32] Siemens. Description of the eigenbeamformer concept (update) and performance evaluation. Technical Report TSGR1#15 R1-01-0203, 3GPP TSG RAN WG 1, 2001.
- [33] Nokia. An extension of closed loop Tx diversity mode 1 for multiple Tx antennas. Technical Report TSGR1#15 R1-00-0712, 3GPP TSG RAN WG 1, 2000.
- [34] W. Utschick. Tracking of signal subspace projectors. 2000. Submitted to *IEEE Transactions on Signal Processing*.
- [35] J. Yang and M. Kaveh. Adaptive eigensubspace algorithms for direction or frequency estimation and tracking. *IEEE Transactions on Acoustics, Speech, and Signal Processing*, 36:241–251, 1988.
- [36] B. Yang. Projection approximation subspace tracking. *IEEE Transactions on Signal Processing*, 43(1):95–107, 1995.
- [37] W. Utschick, M. Treiber, and T. Kurpjuhn. Comparison of two DOA tracking implementations for SDMA. In *Proc. of the Eleventh International Symposium on Personal, Indoor and Mobile Radio Communications*, pages 358–362, 2000.
- [38] M. Treiber, T. Kurpjuhn, and W. Utschick. DSP-implementation of a high-resolution parameter estimating scheme. In *Proceedings of the Third European DSP Education and Research Conference*, 2000.
- [39] E. Tiirola and J. Ylitalo. Performance evaluation of fixed-beam beamforming in WCDMA downlink. In *Proc. 50th IEEE Vehicular Technology Conf. Spring (VTC '00 Spring)*, Tokyo, Japan, May 2000.
- [40] Nokia. Recommended simulation parameters for Tx diversity simulations. Technical Report TSGR1#15 R1-00-0867, 3GPP TSG RAN WG 1, 2000.